coatings

MDPI

Article

Bonding Mechanism of Cold-Sprayed TiO_2 Coatings on Copper and Aluminum Substrates

Noor irinah Omar [1,2,*], Motohiro Yamada [1], Toshiaki Yasui [1] and Masahiro Fukumoto [1]

[1] Department of Mechanical Engineering, Toyohashi University of Technology, 1-1, Tempaku-Cho, Toyohashi, Aichi 441-8580, Japan; yamada@me.tut.jp (M.Y.); yasui@tut.jp (T.Y.); fukumoto@tut.jp (M.F.)
[2] Faculty of Mechanical Engineering and Manufacturing Technology, Universiti Teknikal Malaysia Melaka, Durian Tunggal, Melaka 76100, Malaysia
* Correspondence: Nooririnah@utem.edu.my; Tel.: +60-01-236-61044

Abstract: The cold spraying of ceramic materials is widely acknowledged as a difficult process because it necessitates the feedstock powder particles experiencing a plastic deformation for deposition on a substrate. The problem arises due to the brittle properties of ceramic powder feedstock such as titanium dioxide (TiO_2), combined with a lack of understanding of the bonding mechanisms. In this study, TiO_2 coatings were deposited onto copper and aluminum substrates and the adhesion strength was evaluated to investigate the bonding mechanism. The influence of substrate hardness and remaining surface oxide layer was investigated by annealing the substrates with various temperatures. The results showed that the adhesion strength of the coatings on the aluminum substrate was higher than the copper substrate. Furthermore, the adhesion strength was decreased with increasing the annealing temperature on both substrate materials. These results indicate that a softer aluminum substrate was advantageous for adhesion. Annealing led to thermal softening the substrate; however, the thickness of the surface oxide layer was increased. Therefore, bonding occurred between the cold-sprayed TiO_2 particle and newly deform substrate surface, which yielded the higher adhesion strength. The main bonding mechanism is metallurgical, similarly to the cold-sprayed metallic coatings.

Keywords: cold spray; titanium dioxide; adhesion strength; bonding mechanism; pure copper; pure aluminum

Citation: Omar, N.i.; Yamada, M.; Yasui, T.; Fukumoto, M. Bonding Mechanism of Cold-Sprayed TiO_2 Coatings on Copper and Aluminum Substrates. *Coatings* **2021**, *11*, 1349. https://doi.org/10.3390/coatings11111349

Academic Editor: Alexander D. Modestov

Received: 15 September 2021
Accepted: 1 November 2021
Published: 2 November 2021

1. Introduction

A de Laval nozzle accelerates powder feedstock towards a substrate to deposit a coating, which is known as the cold-spraying process. The sprayed powder impacts on the substrate and forms a thick coating in solid state conditions. The gas temperature should be kept below the melting point of the feedstock powder [1,2]. Thus, the cold spraying of metallic coatings, mechanical interlocking and metallurgical bonding are the most acceptable bonding mechanism theories. Although a substantial amount of work has been carried out to comprehend the bonding mechanism of metallic coatings on metal substrates [3–5], combinations between ceramics and metals are not yet well understood.

In the cold-spraying process, two kinds of metal and ceramic coatings can be formed. To improve mechanical properties, metal matrix composites with ceramic reinforcements can be deposited [6–8].

Cold-spray ceramic metallization has been examined for a range of uses, such as Ti coatings on Al_2O_3 for implant applications, to tackle the ceramic's low toughness [9]. Furthermore, porous materials are used for a variety of applications, such as the dry-freezing method for the synthesis of TiN nanoparticles for Li–S battery applications [10]. The hexagon-like 2D structure of CoMoO4@CFC possesses mesoporous properties with abundant electroactive sites as a charge storage host [11], and for enhanced supercapacitor (SC)

electrode efficiencies, a simple hydrothermal approach has been employed to easily produce unique floral CoNi2S4 nanoneedle assemblies (CNS-NAs) on Ni foam [12].

However, the cold spraying of pure ceramic powder such as TiO_2 without any binder on a metal substrate has not been extensively explored to date. The cold spraying of thick and pure TiO_2 on metal substrates has been reported in previous investigations [13–17]; however, the mechanism of bonding of cold-sprayed TiO_2 on metal substrates is unknown.

Several findings from experiments regarding the impact of the substrate properties on the mechanisms of bonding of cold spraying ceramic have been published. Winnicki et al. used amorphous and crystalline TiO_2 powders cold-sprayed onto aluminum and steel substrates with varying surface roughness values. They discovered that the grit-blasted substrate enabled them to reduce defects caused by differences in metallic substrates and ceramic coating properties, which were influenced by the thermal expansion coefficient. The bonding mechanism relied on mechanical interlocking [18].

TiO_2 particles were cold-sprayed onto a polished titanium surface. Schmidt et al. discovered that when a substrate is deformed plastically, a large unbroken unity area forms between the particles and the substrate, resulting in long-lasting bonding [19]. Kliemann et al. cold-sprayed TiO_2 particles onto steel, copper, titanium and aluminum magnesium sulfate substrates. The dominant bonding system among the particles and the substrate was identified as a ductile substrate that allowed shear instabilities to occur [20]. Gutzmann et al. investigated the deposition of various particles on substrates of different temperature and gained a better understanding of the impact morphology of single TiO_2 particles. They demonstrated that concentric rings, such as in the shear instability zone, existed on the impacted substrates. Only when the substrate temperature exceeded a certain limit could a single TiO_2 particle be deposited. It has been proposed that preheating the substrates softens them and facilitates substrate shear instability, thereby facilitating coating deposition [21]. Gardon et al. reported that between the particles and a stainless-steel substrate, chemical bonding caused TiO_2 formation on the substrate during the cold-spraying procedure. They demonstrated that the existing layer of titanium sub-oxide provides the substrate with the required surface coarseness for TiO_2 particles to form a coating. Furthermore, the surface formation is critical for deposition because it can contribute chemical compatibility as particle engagement following an impact. The hardness of the substrate can facilitate particle–substrate synergy [22].

Based on previous reports, material properties have a crucial role in the formation of ceramic coatings with the cold spray method. However, specifications of the bonding mechanism are still unknown, which are essential to understand the bonding mechanism to improve the adhesion strength and reliability of the coatings. Therefore, this study examined the effect of substrate hardness and a surface oxide layer on the adhesion strength of TiO_2 coatings. Pure copper and pure aluminum were chosen, which are often used as coating and substrate materials in the cold-spray process.

2. Materials and Process

2.1. Process

Cold-spraying equipment with a De-Laval 24TC nozzle (CGT KINETIKS 4000; Cold Gas Technology, Ampfing, Germany) was utilized in all coating experiments. Nitrogen at a temperature of 500 °C and 3 MPa pressure was used as a gas. The spray distance was 20 mm, with a process traverse speed of 10 mm/s. The powder feed rate was three grams per minute, and the pass number was one.

2.2. Materials

We used agglomerated TiO_2 powder with a pure anatase crystalline structure (TAYCA Corporation, WP0097, Osaka, Japan) as a feedstock, which consisted of a pure anatase crystalline structure with an even grain size of 7.55 microns.

Pure copper (C1020) and pure aluminum (AA1050) were used as the substrates. The substrates were first grit-blasted, then annealed, to investigate the effect of surface oxidation at each temperature. The annealing was carried out with an electric furnace at four temperatures (i.e., 100 °C, 200 °C, 300 °C, and 400 °C) under ambient atmospheric conditions. Substrates were annealed in an electric furnace at different temperatures, with increases of 15 °C/5 min; later, after soaking for five minutes, the substrates were cooled to room temperature in the furnace. A schematic diagram of the electric furnace and temperature increments are shown below in Figure 1. Annealing is a heat treatment process that changes material properties to make it more workable by enhancing ductility and reducing hardness [23].

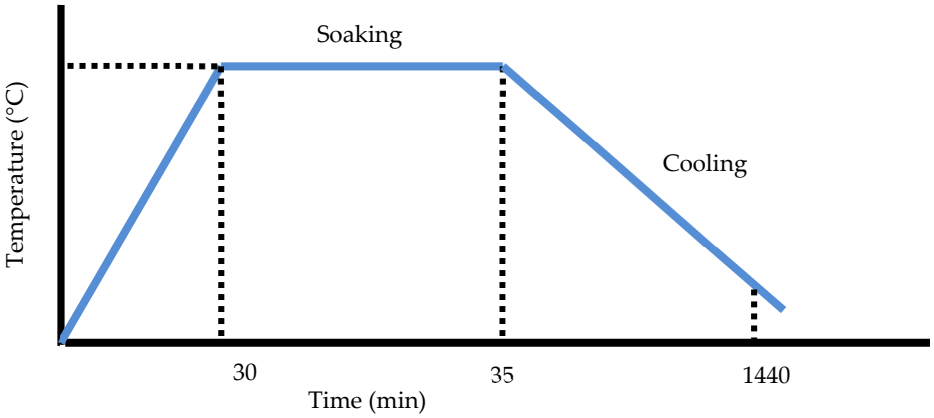

Figure 1. Schematic of annealing temperature increment process.

The annealed substrates were sprayed at room temperature in all experiments. Substrates without annealing (room-temperature substrate) were also used in this study. For further understanding the influence of substrate oxidation, we also cold-sprayed a titanium dioxide coating annealed at 400 °C with grit blasting to eliminate the oxide film grown on the substrate surface before the cold-spraying process. The material chemical distributions of the substrates used are given in Table 1.

Table 1. Material chemical distribution [wt.%].

	Cu	**P**	**Mn**	**Zn**	**Sn**	**Ni**	**Co**	**Zr**	**Ag**
C1020	Bal	0.04	1.1	0.1	0.72	0.06	0.21	0.05	0.04
	Al	**Fe**	**Si**	**Zn**	**Cu**	**Mn**	**Mg**	**Ti**	**Other**
AA1050	Bal	0.40	0.25	0.05	0.05	0.05	0.05	0.05	0.03

2.3. Characterization

2.3.1. Strength Testing

In accordance with JIS H 8402, specimen areas of Ø25 mm × 10 mm were used to check the coatings' adhesion strength, which was provided as the fracture load amount measured by a universal testing machine (Autograph AGS-J Series 10 kN, Shimadzu, Japan). For each spraying condition, we examined the adhesion strength with a median of five specimens. EDX was conducted on the fracture coating surface.

2.3.2. Coatings Evaluation

The cross-sectional microstructures of the TiO_2 coating on annealed substrates were examined using a scanning electron microscope (SEM: JSM-6390, JEOL, Tokyo, Japan).

2.3.3. Micro Vickers Hardness

The substrate hardness was examined with an HMV g micro Vickers hardness tester to study the relationship between the hardness of the annealed substrate surface and the coating strength (Shimadzu, Japan). The hardness examined was HV 0.1 with a test force on the cross section of 98.07 mN at a dwell time of 10 s. The representative micro-hardness value was the median of 5 tests conducted on each substrate at roughly the same point.

2.3.4. Substrate Oxide Layer Evaluations

The thickness of the substrate oxide layers was measured using X-ray photoelectron spectroscopy (ULVAC-PHI, PHI Quantera SXM-CI, Kanagawa, Japan). In this study, XPS data for Cu2 p3/2, Al 2p, and O 1s were collected using a monochromatic Al K source (15 mA, 10 kV) with narrow scans (0–1000 eV) for various annealed substrates. Subsequently, the examined binding energies were corrected with C 1s at 285.0 eV and pre-sputtering to clean the surface and prevent it affecting the substrate surface and the measurements; XPS analysis was conducted without pre-sputtering. The XPS testing parameters for pure metal oxide films are shown in Table 2.

Table 2. XPS parameter of pure metals oxide film testing.

Measured Regions	Cu2 p3/2, Al 2p, O 1s
Examined X-ray output (W)	10
Probe diameter (μm)	50
Time per step (ms)	30
Pass energy	140
Cycle	30

2.3.5. Oxide Surface Roughness

NanoWizard® 3 Atomic Force Microscope (JPK Instruments, Bruker, Billerica, MA, USA) were used to analyzed oxide surface roughness with scan area of 5 μm using areal scanning method.

2.3.6. Single-Particle Deposition

Single-particle deposition was carried out to study the changes which occur on a high-velocity single particle impacted on different sort of substrates. To perform single-particle deposition of TiO_2 on pure materials annealed at 400 °C, a CGT Kinetiks 4000 cold-spray system with a specially built suction nozzle was used. Before the deposition, the pure materials were ground and polished until they had a mirror finish. The temperature was 500 °C, and pressure of the process gas (nitrogen) was 3 MPa. The nozzle's outlet length from the substrate was set to 20 mm. The process moved at a rate of 2000 mm/s. The sample was washed in acetone before spraying. To study the relationship between the single TiO_2 particle bonding behavior and the annealed mirror-polished pure materials, FEI Helios Dual Beam 650 field emission SEM (FESEM, FEI, Hilsboro, OR, USA) and focused ion beam (FIB, FEI, OR, USA) microscopes were used.

2.3.7. Transmission Electron Microscopy Testing

A single TiO_2 particle was deposited on 25 × 25 × 5 mm^3 room-temperature and mirror-polished C1020 and AA1050 annealed at 400 °C. By using focused ion beam (FIB) milling equipment, thin membrane films for transmission electron microscopy (TEM) testing were thoroughly prepared from collected titanium dioxide particles at room temperature and mirrored pure metal substrates annealed at 400 °C (FEI Helios Dual Beam 650). In addition to sample preparation, a thin film was created and examined using field emission gun (FEG) electron microscopy on EOL JEM-2100F FE-TEM apparatus in scanning mode at 200 kV. TEM line analysis was used to investigate atomic concentration changes.

3. Results

3.1. Titanium Dioxide Coating Microstructure on Annealed Pure Metals

Figure 2a–d reveals the titanium dioxide coating cross-sectional microstructure on C1020 and AA1050 substrates after 400 °C annealing at room temperature. The images show that dense coatings with a thickness around 300 μm could be obtained on a room-temperature substrate, meaning that a critical velocity was achieved for these materials. This explains that titanium dioxide coatings attached to the pure room temperature materials better than the annealed substrates. Large cracks between the coating and the annealed substrates were observed, as shown in Figure 2b,d. However, cracks did not form on the room-temperature substrates at the interface. It can be considered that the substrate annealing prior to the spraying reduces the adhesion by the titanium dioxide coating cold-spraying method and the pure metals.

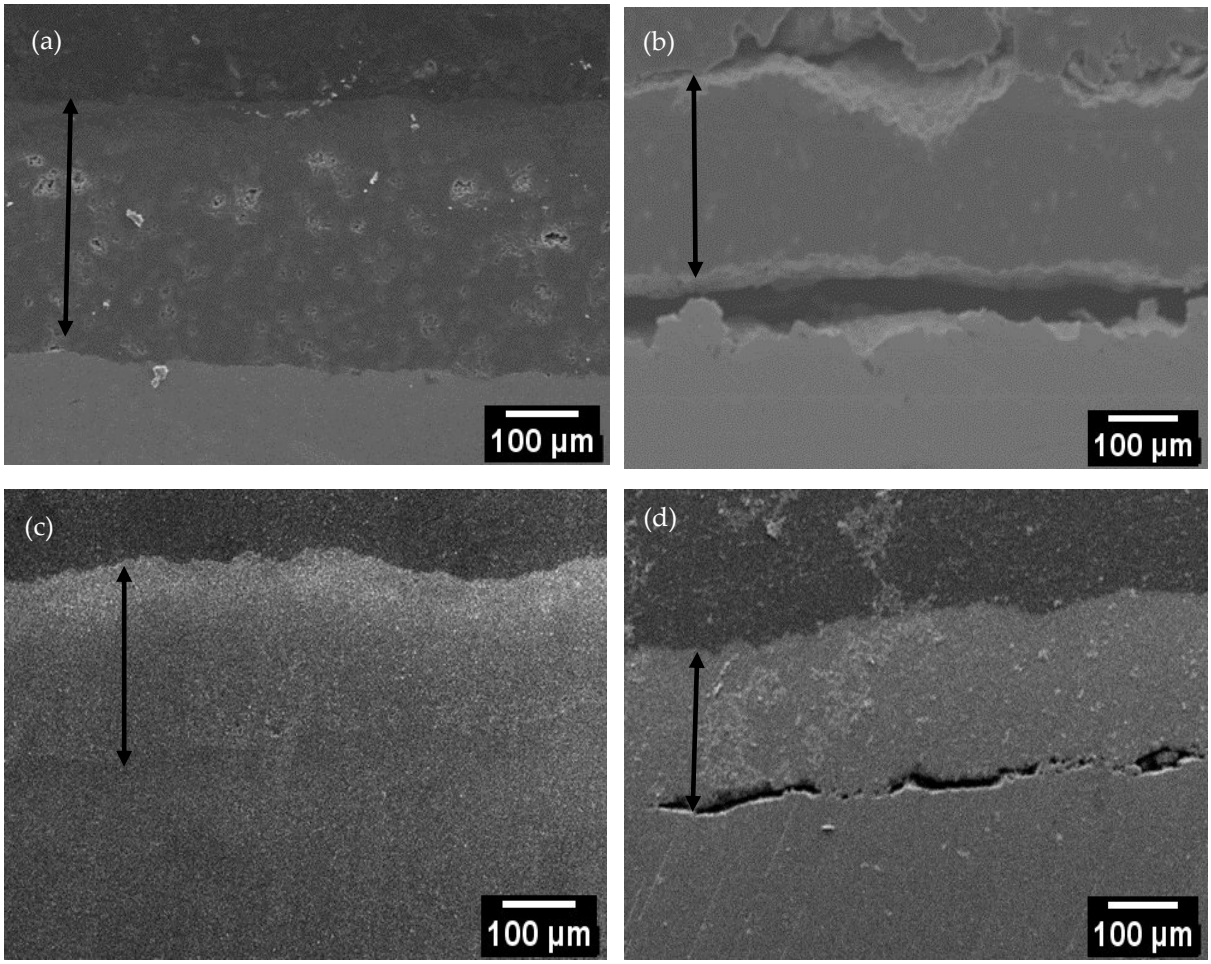

Figure 2. Cross-sectional microstructure of titanium dioxide coating on C1020 (**a**) at RT and (**b**) annealed at 400 °C. AA1050 (**c**) at room temperature and (**d**) annealed at 400 °C.

The spraying parameters were constant for all experiments. Therefore, the substrate material and annealing did not strongly affect the deposition efficiency of the titanium dioxide cold-spraying coating method. The cold-spraying procedure is divided into two phases, adhesion and cohesion bonding. The first stage is the deposition of an interlayer between the pure metals and the particle. This can affect the deposition behavior of the first layer, although the deposition efficiency of the coating is mainly affected by cohesion between the particles. The effect of the substrate conditions can be ignored.

3.2. Strength of Adhesion

Figure 3 shows the coating strength of titanium dioxide upon C1020 and AA1050 substrates at various annealing temperatures. Both pure metals revealed a decreasing tendency of the coating strength with the increasing annealing temperature. Furthermore, the adhesion strength of the AA1050 substrate was higher than the C1020 substrate for all annealing conditions. The coatings sprayed upon the C1020 substrate at 400 °C automatically peeled off during the specimen preparation. EDS mappings, illustrated in Figure 4, show that the elements present are copper (Cu), titanium (Ti), oxygen (O) and carbon (C) for the fractured coating of titanium dioxide on the annealed copper substrate. This EDS mapping showed that a small part of the copper substrate is embedded on the TiO_2 coating. Figure 5 shows that the elements present are aluminum (Al), titanium (Ti), oxygen (O) and carbon (C) for fractured coating of titanium dioxide on annealed aluminum substrate. This EDS mapping showed that also a small part of aluminum substrate is embedded on the TiO_2 coating.

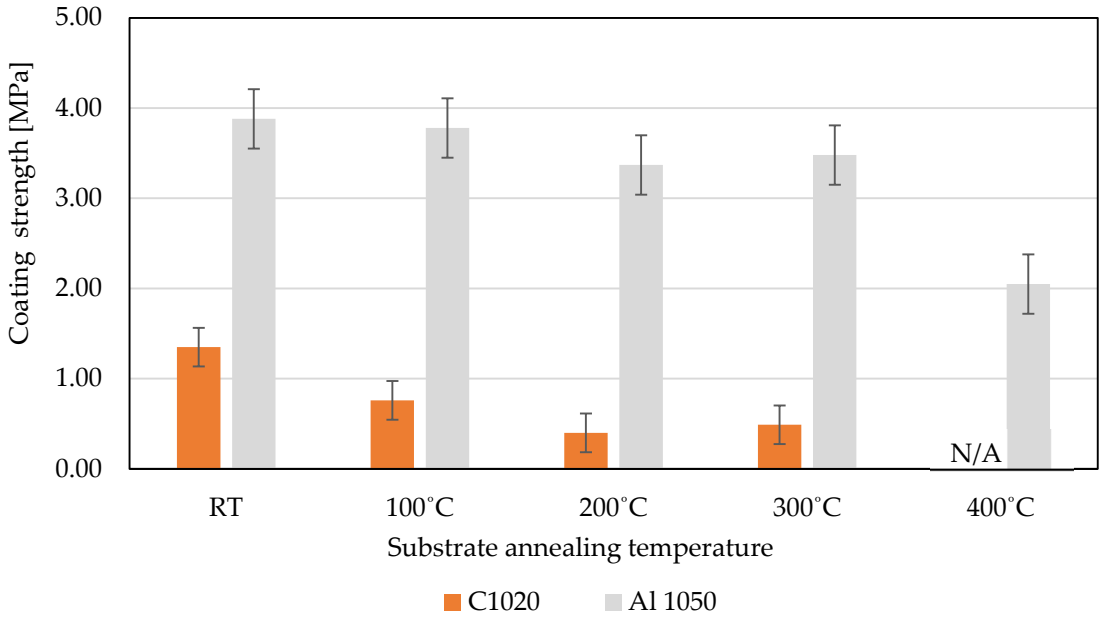

Figure 3. Coating strength of the TiO_2 on C1020 and AA1050 from RT to a 400 °C annealing temperature.

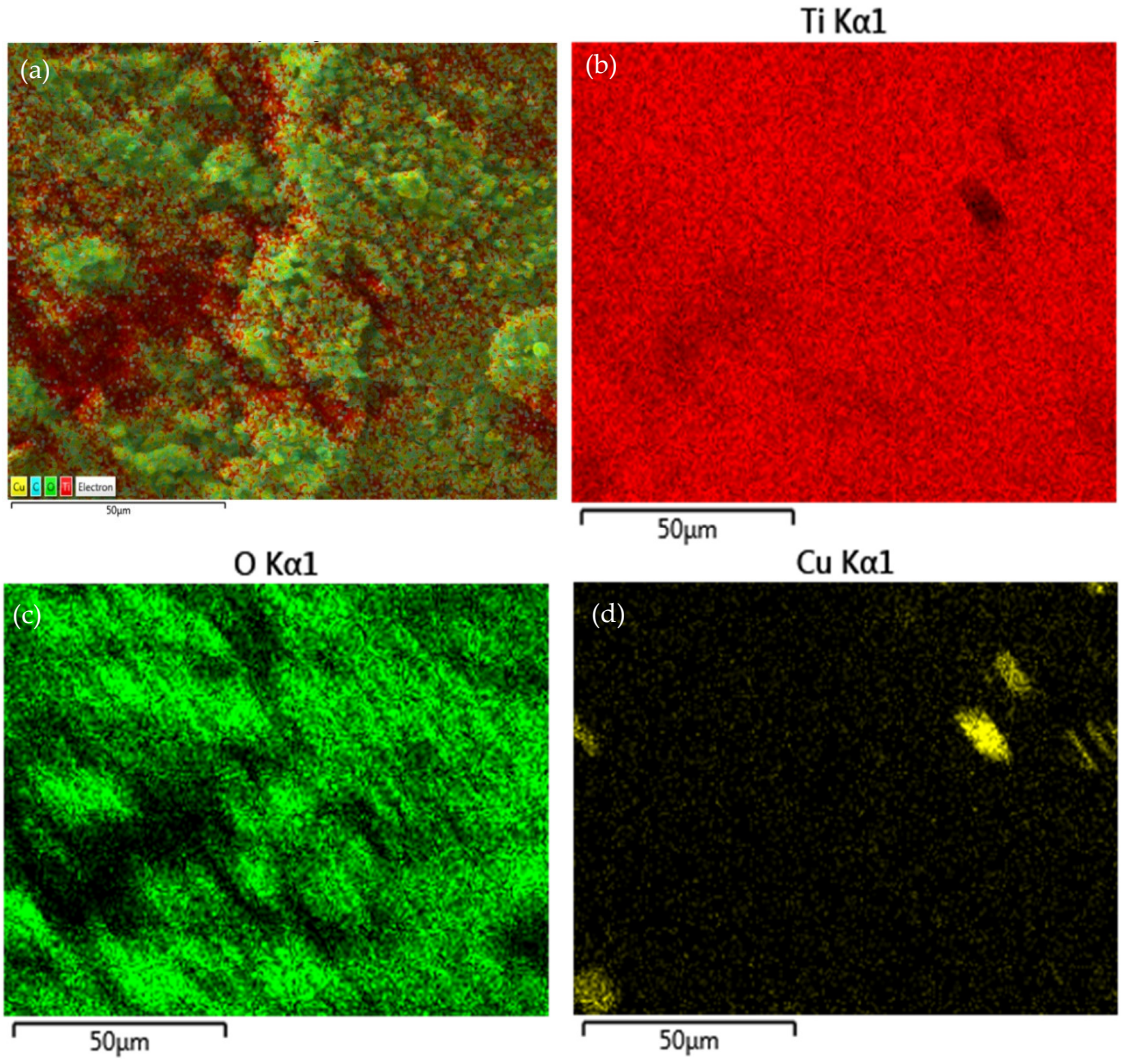
(a)
Cu C O Ti Electron
50µm
Ti Kα1
(b)
50µm
O Kα1
(c)
50µm
Cu Kα1
(d)
50µm

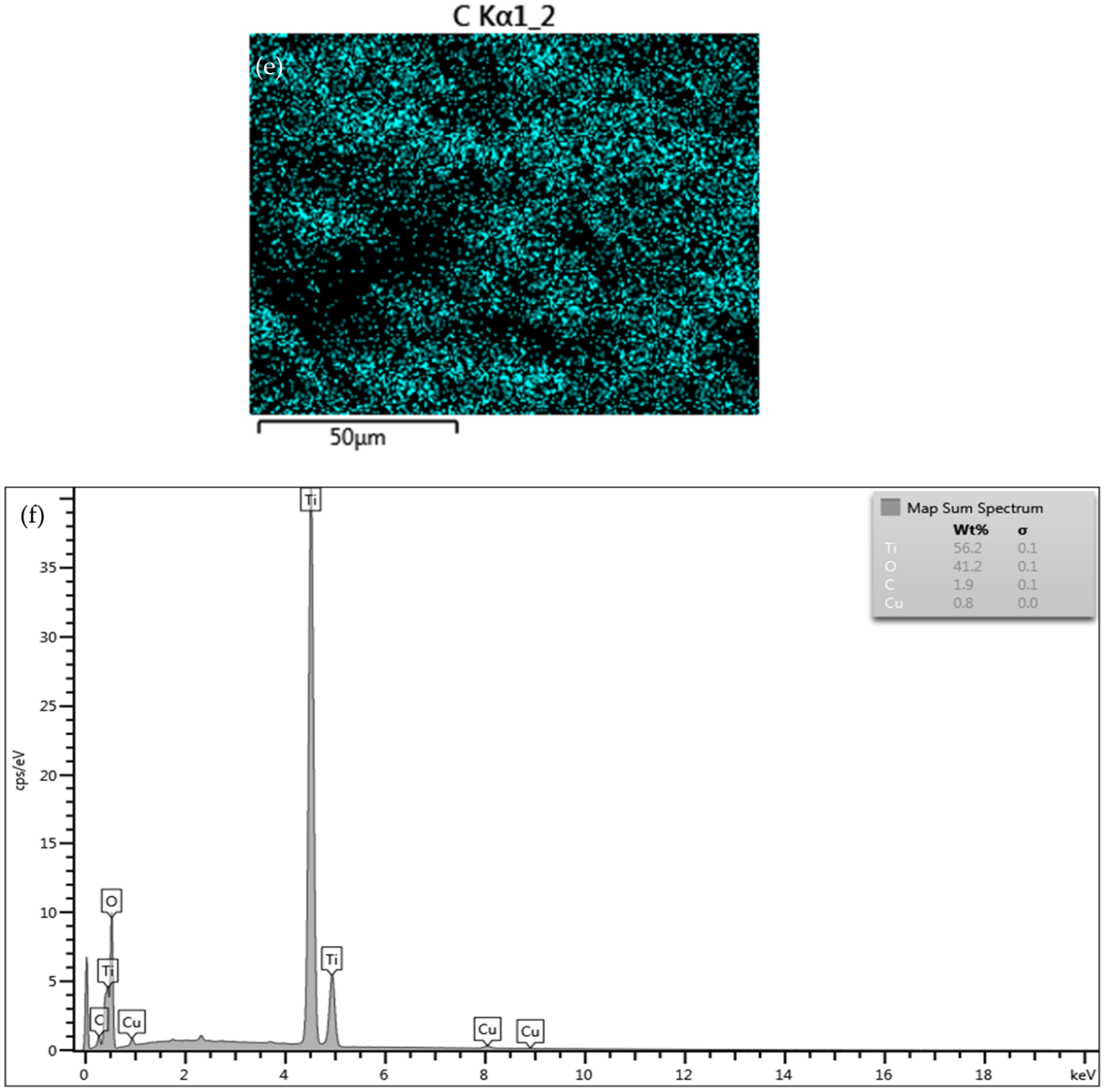

Figure 4. EDX elemental mappings of TiO_2/annealed C1020 fracture coating: (**a**) SEM; (**b**) titanium; (**c**) oxygen; (**d**) copper; (**e**) carbon; (**f**) map sum spectrum.

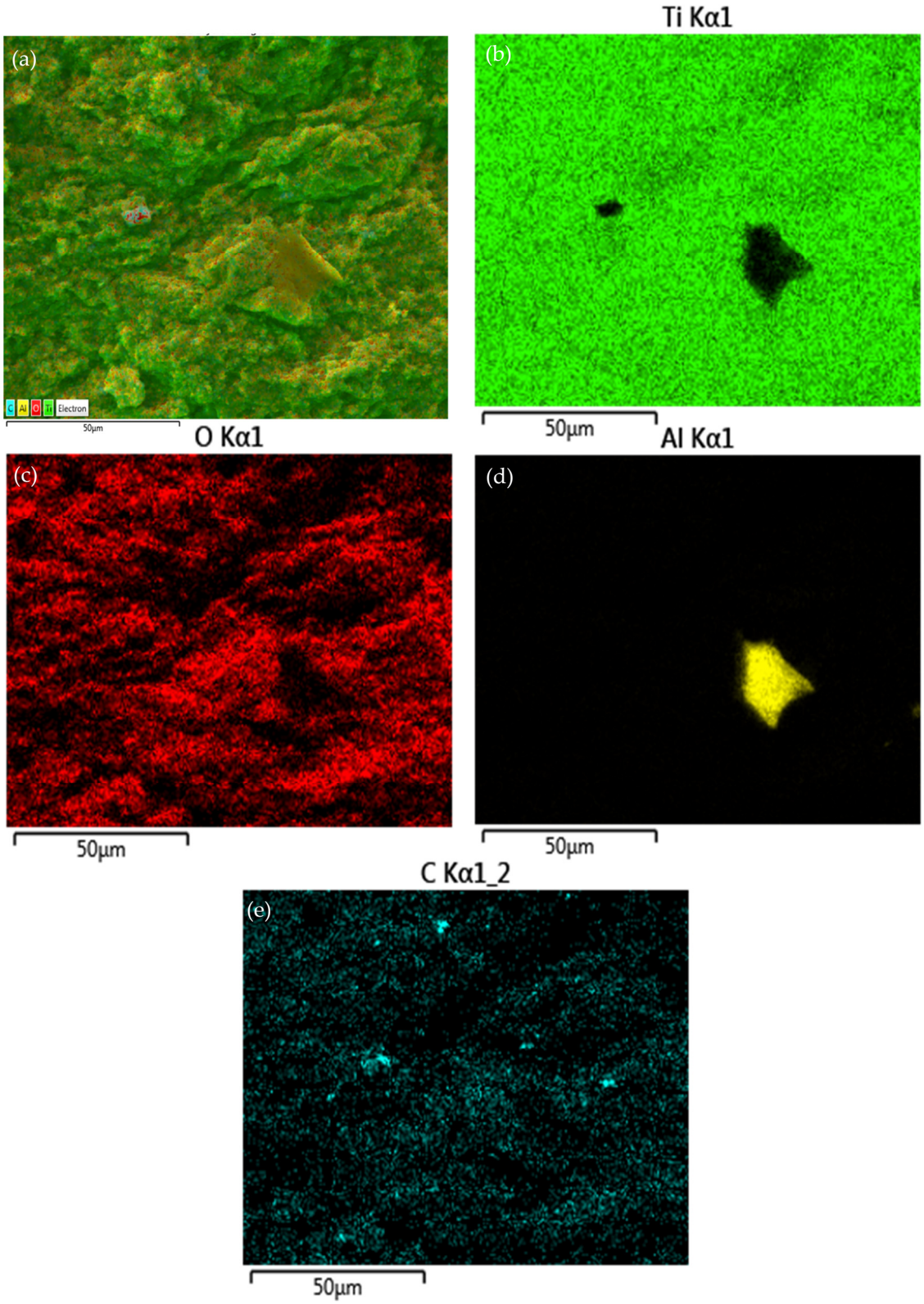
(a)
C Al O Ti Electron
50µm
Ti Kα1
(b)
50µm
O Kα1
(c)
50µm
Al Kα1
(d)
50µm
C Kα1_2
(e)
50µm

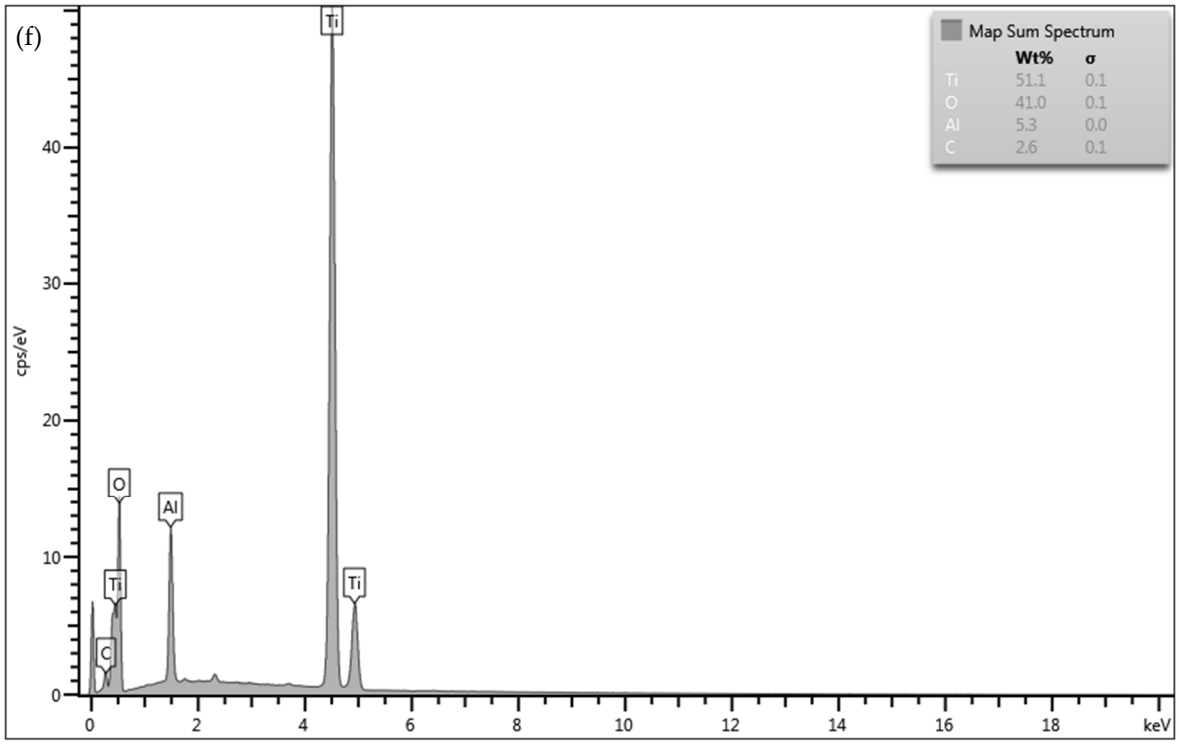

Figure 5. EDX elemental mappings of TiO_2/annealed AA1050 fracture coating: (**a**) SEM; (**b**) titanium; (**c**) oxygen; (**d**) aluminum; (**e**) carbon; (**f**) map sum spectrum.

Increasing the annealing temperature for C1020 and AA1050 from RT to 400 °C indicated the massive deposition of an oxide film on the pure metal surface, changing the substrate hardness. It is vital to understand how this factor influences the trend in the coating strength upon these substrates to find out more regarding the bonding mechanism involved.

3.3. Depth Profile of the Oxide Layer

Figures 6 and 7 show the XPS evaluations of the in-depth room temperature substrates and substrates annealed at 400 °C for C1020 and AA1050 substrates, respectively. In situ argon ion beam sputtering can be used to analyze the distribution as a function of depth. Figure 6a–e shows that the atomic concentration of oxygen in the innermost part of the oxide film was raised significantly as the temperature of the annealing material rose from room temperature to 400 °C. Figure 7a–e shows that oxygen levels in the deepest part of the AA1050 increased from room temperature to 400 °C.

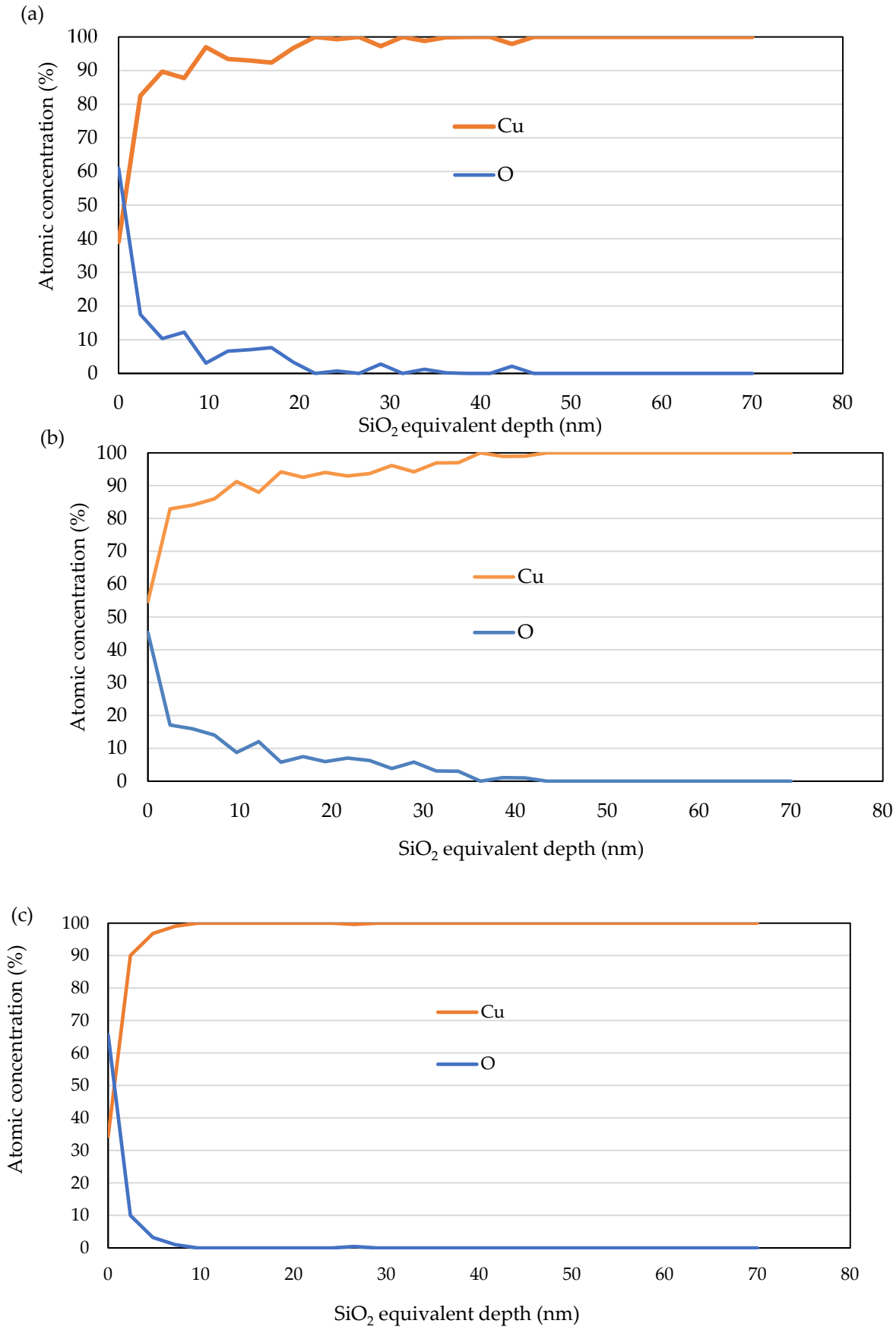
(a)
Atomic concentration (%)
100
90
80
70
60
50
40
30
20
10
0
Cu
O
0
10
20
30
40
50
60
70
80
SiO2 equivalent depth (nm)
(b)
Atomic concentration (%)
Cu
O
SiO2 equivalent depth (nm)
(c)
Atomic concentration (%)
Cu
O
SiO2 equivalent depth (nm)

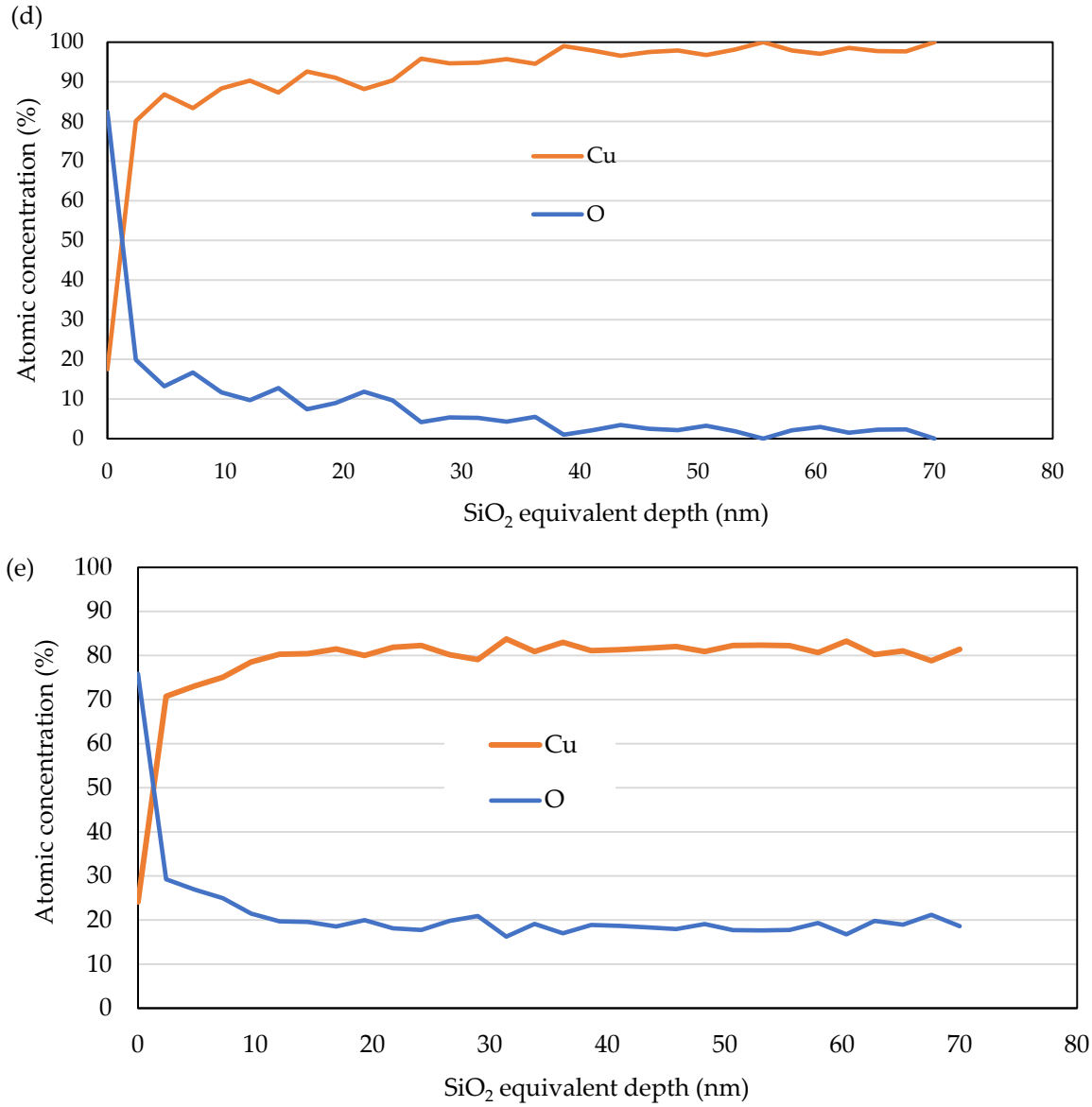

Figure 6. Depth profile analysis of C1020 (**a**) at RT, (**b**) annealed at 100 °C, (**c**) annealed at 200 °C, (**d**) annealed at 300 °C, and (**e**) annealed at 400 °C.

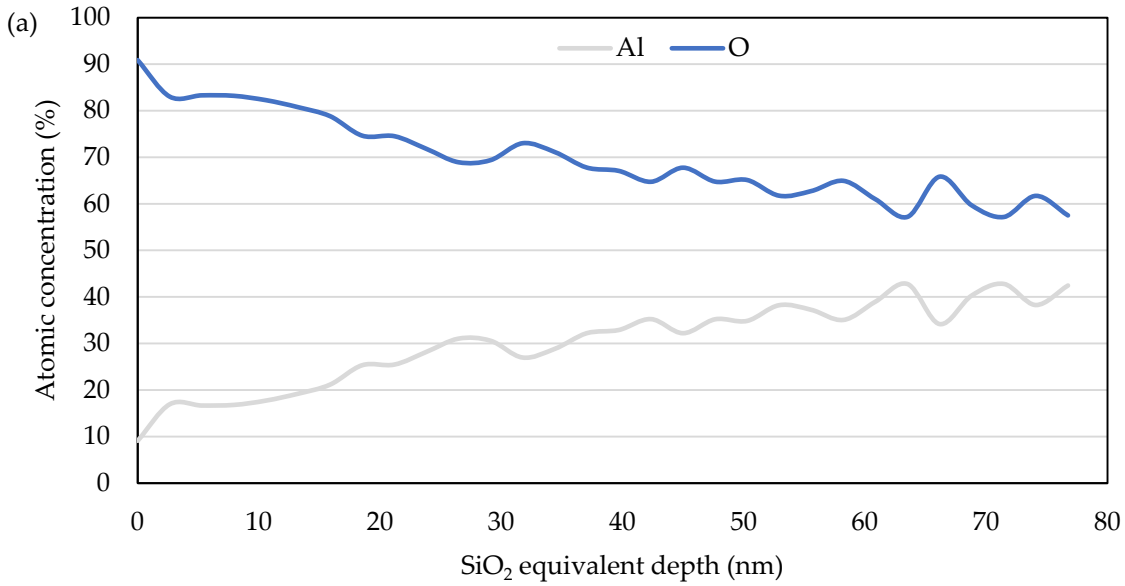
(a)
Al
O
Atomic concentration (%)
100
90
80
70
60
50
40
30
20
10
0
0
10
20
30
40
50
60
70
80
SiO2 equivalent depth (nm)

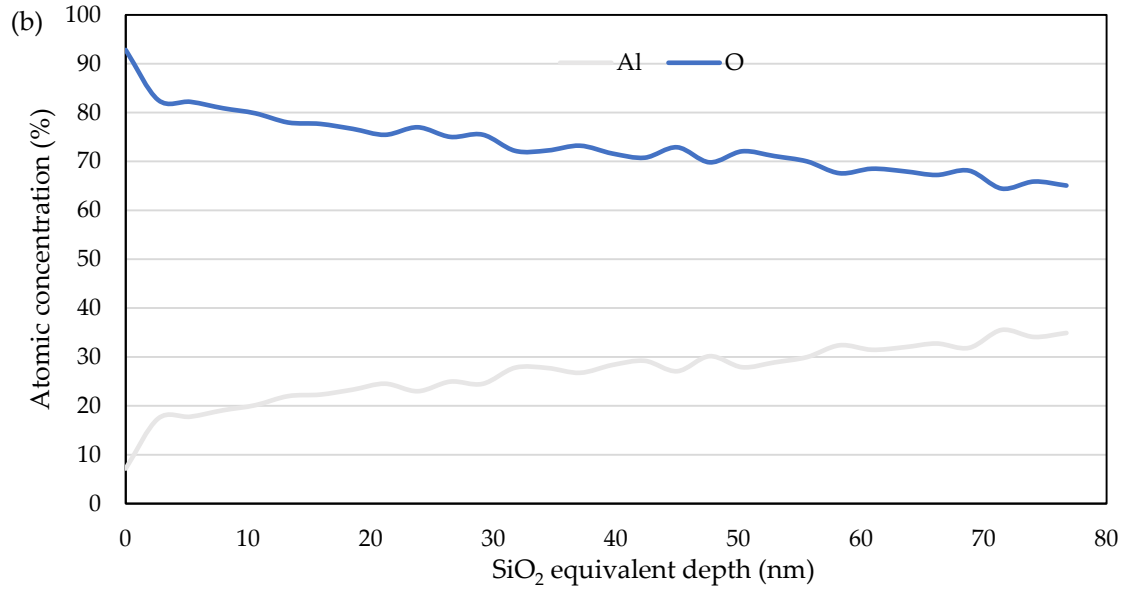
(b)
Al
O
Atomic concentration (%)
100
90
80
70
60
50
40
30
20
10
0
0
10
20
30
40
50
60
70
80
SiO2 equivalent depth (nm)

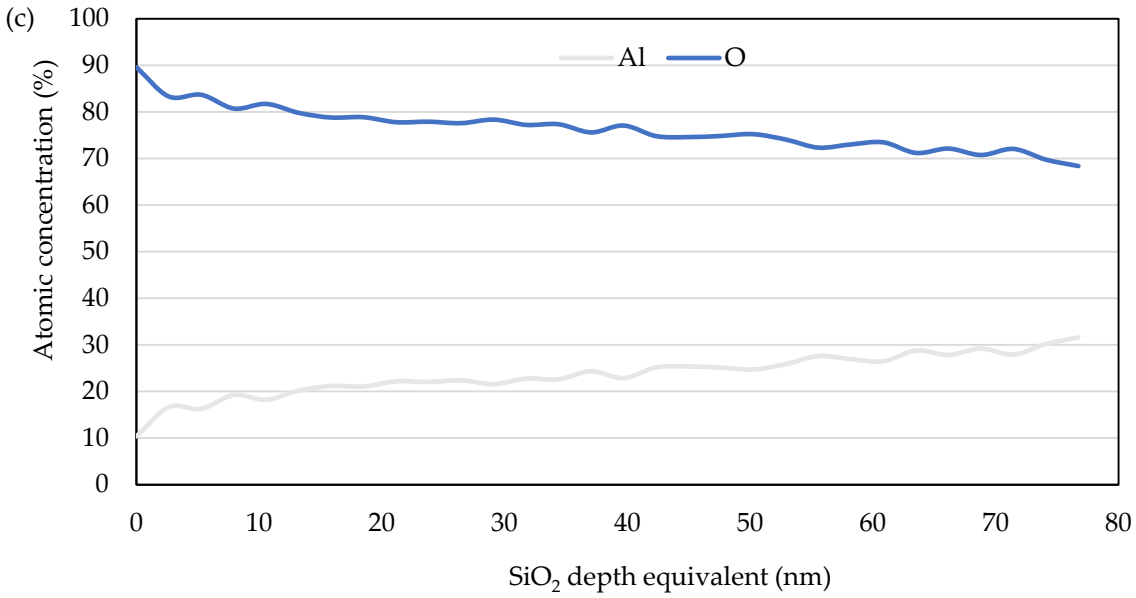
(c)
Al
O
Atomic concentration (%)
100
90
80
70
60
50
40
30
20
10
0
0
10
20
30
40
50
60
70
80
SiO2 depth equivalent (nm)

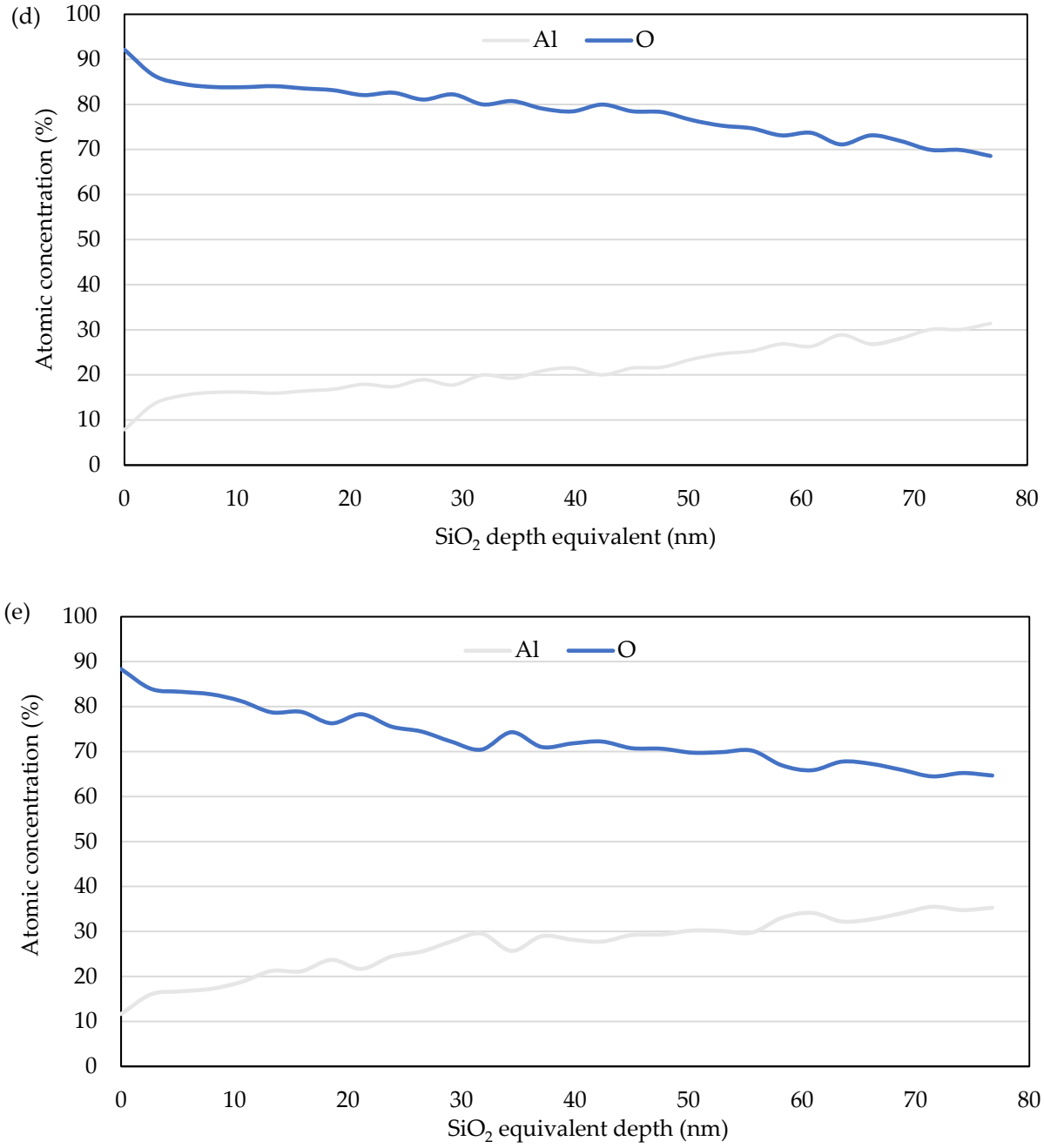

Figure 7. Depth profile analysis of AA1050 (**a**) at RT, (**b**) annealed at 100 °C, (**c**) annealed at 200 °C, (**d**) annealed at 300 °C, and (**e**) annealed at 400 °C.

This indicates that as the annealing temperature rises, the oxide layer of both pure materials thickens. Referring to Li et al., as the oxide film thickness increases, greater kinetic energy is required to remove the oxide layer, and bond formation also requires a higher flow rate of particle. Alternatively, under the same particle impact conditions [24], the effective bonding area decreases [24]. The particle velocity remained unchanged throughout all conditions in this process, which might clarify why the bonding strength of a TiO_2 coating on the heat-treated surfaces of both materials significantly reduced as the temperature was increased from room temperature to 400 °C.

3.4. Oxide Surface Roughness

Figures 8 and 9 show the 2D oxide surface roughness of C1020 and AA1050 at RT and materials annealed at 400 °C. Both pure metals showed an increasing trend in oxide surface roughness as the annealing substrate temperature was increased: 13.89 nm (RT) to 45.02 nm (400 °C) for C1020, and 20.56 nm (RT) to 121.9 nm (400 °C) for AA1050. The influence of substrate surface roughness in terms of oxide roughness can be summarized as follows: in softer substrate materials such as copper and aluminum, a larger surface roughness gives higher adhesion strength inversely to annealing temperature increases.

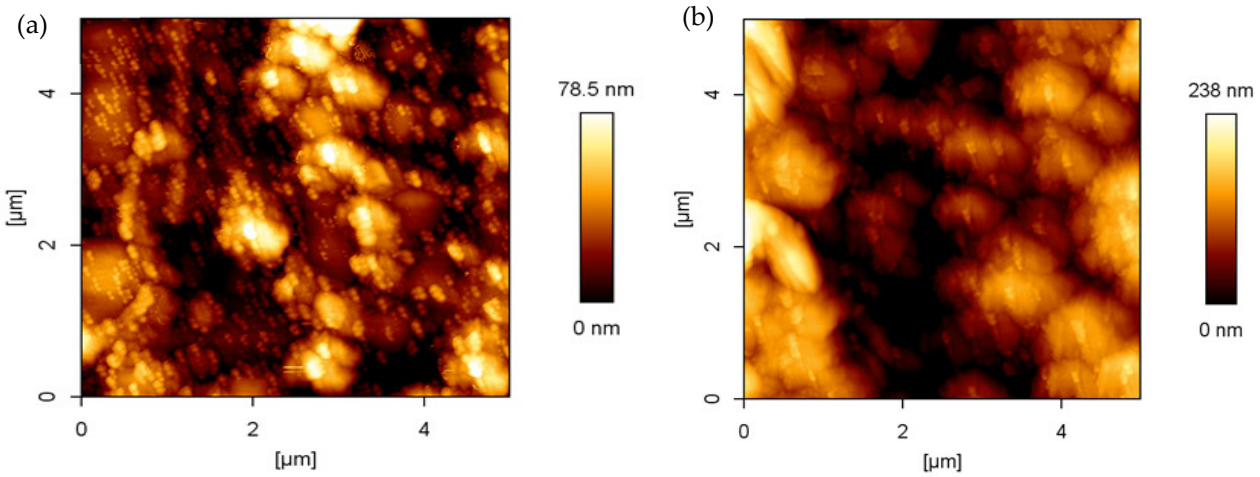

Figure 8. Oxide surface roughness of C1020 (**a**) at RT and (**b**) annealed at 400 °C.

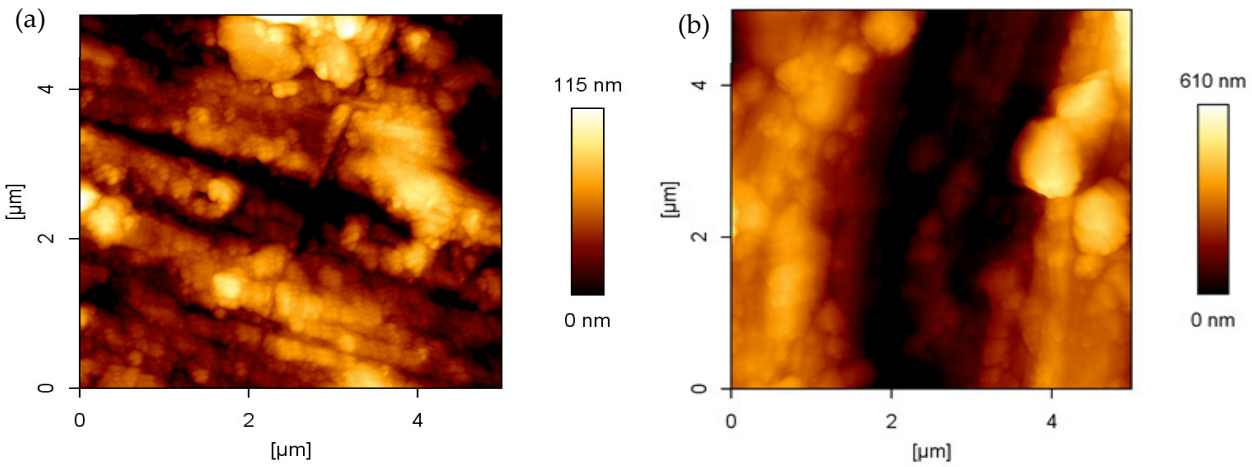

Figure 9. Oxide surface roughness of AA1050 (**a**) at RT and (**b**) annealed at 400 °C.

Metallic interlocking is involved in coating deposition, substrate coarseness and increases deposition qualities, as per some studies conducted [5,25–27]. According to reports, grit-blasted substrates have a greater adhesion capacity because they have a wider surface contact and mechanical interlocking [25]. The surface roughness of annealed substrates in terms of oxide roughness is not directly influenced by the titanium dioxide coating adhesion strength to heated base materials. Therefore, other stimuli may exist and need to be clarified to understand the bonding mechanisms involved.

3.5. Pure Metal Vickers Microhardness

Figure 10 shows the heat-treated pure metal hardness values of C1020 and AA1050 from RT to 400 °C. C1020 showed a declining tendency from 103.2 Hv (RT) to 45.96 Hv (400 °C), and AA1050 also showed a decreasing trend from 45.36 Hv (RT) to 27.7 Hv (400 °C), which is almost a 50% reduction in the substrate hardness.

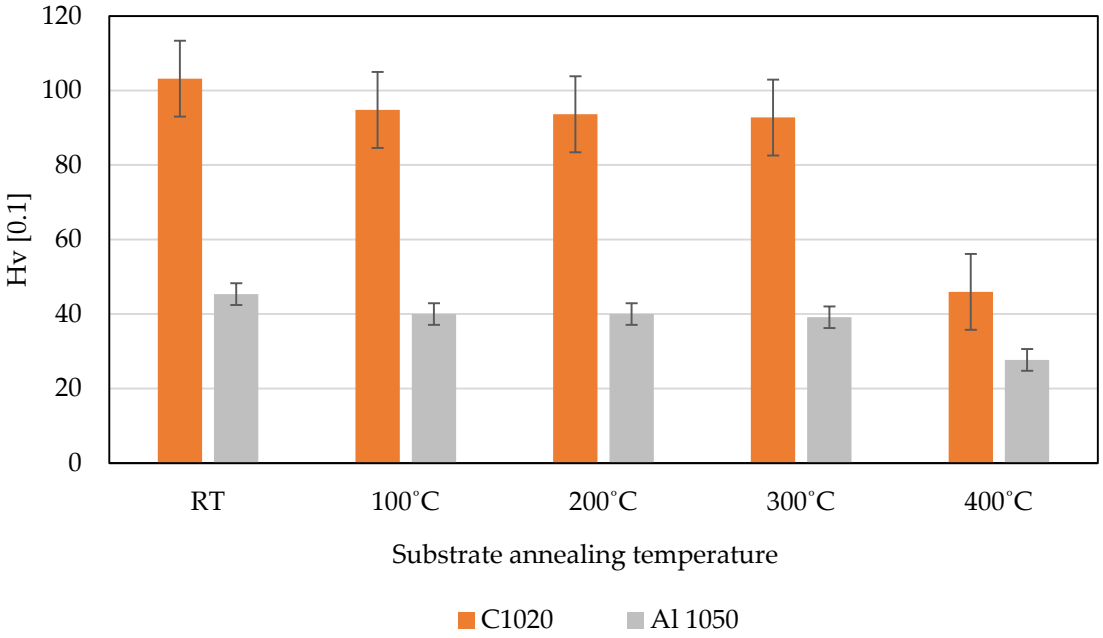

Figure 10. Heat-treated pure metal hardness of both pure materials from RT to 400 °C.

Annealing heat treatments alter the characteristics of materials. The primary goal of annealing is to increase the ductility of a metal while decreasing its hardness [23]. The kinetic progression of pure copper micro-hardness after isothermal recrystallization proceeds at 250, 300, and 380 °C. The recovery process causes a modest decrease in microhardness during the incubation period. Then, a large fall in HV from HV = 100 (at the initial cold-rolled phase) to HV = 50 (at the fully recrystallized phase) confirms recrystallization [28].

C1020 and AA1050 recrystallization at 400 °C and prolonged cooling in an electric furnace with air as a medium allows grains to grow bigger and reduces substrate hardness, leading to softer pure materials. Annealed substrates become softer at 400 °C due to the recrystallization process; therefore, when high-velocity cold-sprayed TiO_2 impacts the substrate surface, substrate deformation is expected and will lead to the increased adhesion bonding of TiO_2 coatings; however, the coating strength of titanium dioxide on both pure materials was lowest at the 400 °C annealing temperature. As a result, substrate deformation (mechanical anchoring) is not one of the most essential aspects influencing titanium dioxide coating adhesion bonding on annealed C1020 and AA1050.

3.6. Focus Ion Beam Single Particle Titanium Dioxide on Pure Metals Annealed at 400 °C

The top view and cross-sectional images of the titanium dioxide particles impacting on C1020 and AA1050 annealed at 400 °C are shown in Figure 11a–d. The objective of this wipe test was to study more about how TiO_2 particles adhere to annealed pure metal substrates. Only C1020 and AA1050 annealed at 400 °C were selected because they had the thickest oxide film. As demonstrated in Figures 11a,b, the TiO_2 particle remained intact following the collision, whereas the base surface of the C1020 annealed at 400 °C deformed due to impacting during the cold-spraying process.

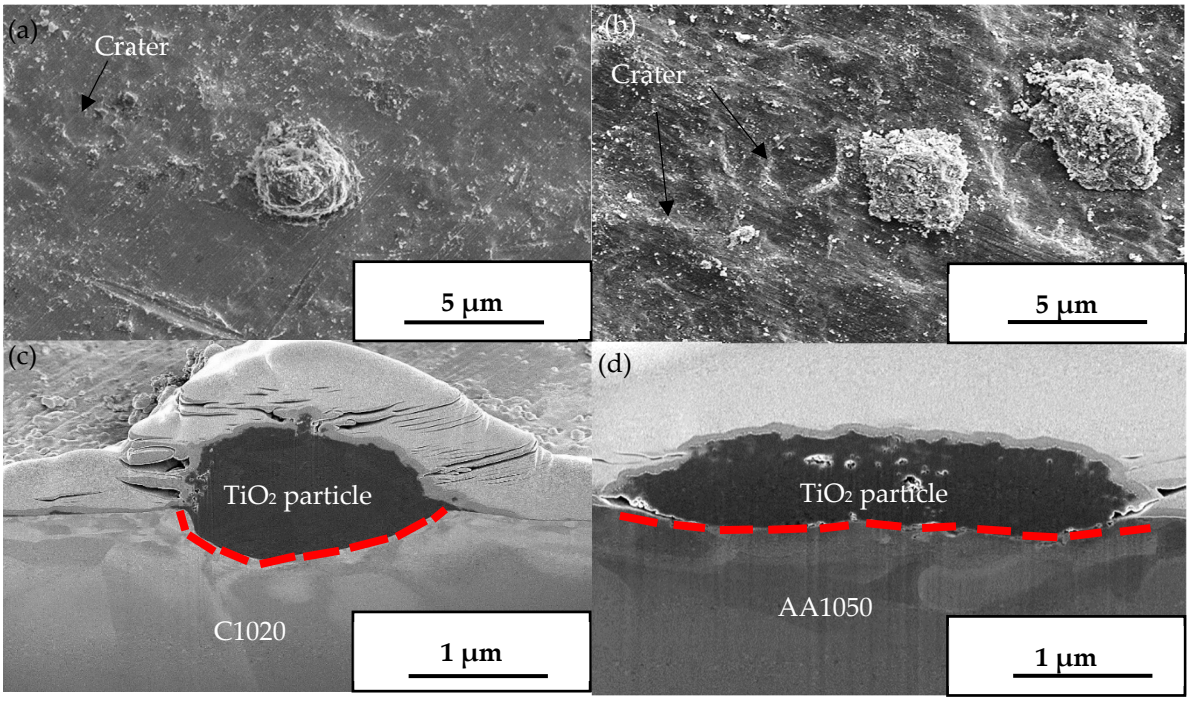

Figure 11. SEM images of the TiO_2 particle on (**a**) C1020 annealed at 400 °C, (**b**) AA1050 and cross-sectional images of titanium dioxide particle on (**c**) C1020 and (**d**) AA1050 heat-treated at 400 °C.

Moreover, on soft substrates such as aluminum, TiO_2 particles deformed. The TiO_2 particles collided with the substrate with minimum deformation and rebounded, producing craters on the surface. The arrow in Figure 11 depicts this. For soft surfaces, impacting energy generated during the spraying process is also utilized for surface deformation, according to Ernst et al. [29]. The craters were deeper and suffered severe damage because of the decreased hardness of aluminum annealed at 400 °C due to recrystallization, as indicated in the SEM images in Figures 11b–d.

Both substrates underwent substrate deformation after being impacting by high-velocity, cold-sprayed TiO_2 particles, as shown by the red dotted line in the figure below. The adhesion strength of the coatings showed a decreasing tendency as the temperature of the heat-treated base material was increased. This implies that substrate deformation or mechanical anchoring are not factors influencing the adhesion bonding of C1020 and AA1050 annealed at 400 °C with a TiO_2 coating. Ichikawa et al. reported that a thicker oxide film hinders the establishment of a new surface, and oxide layers serve as a deposition barrier for cold-sprayed CoNiCrAlY on an Inconel 625 substrate. Oxide films have a major impact on the deposition process [30]. The same author also reported that the south pole is the middle of a single crater, which is covered by an oxide film coating, and hence, is not bonded. At the tip of each crater, however, an oxide-free metallic region can be observed, allowing a strong bond to form between cold-sprayed copper deposited on the aluminum substrate [31]. Our experiment is consistent with the results of Ichikawa et al., where substrate deformation existed on both pure metals annealed at 400 °C, but the adhesion strength was lowest at this annealing temperature due to the oxide film remaining on the substrate surface after impact from cold-sprayed TiO_2 particles.

3.7. Transmission Electron Microscopy Investigation of the Oxide Film Interface between TiO_2 Particles and Substrates at Room Temperature and Annealed at 400 °C

Figure 12 is TEM images of the interface between a single TiO_2 particle and C1020 and AA1050 annealed at 400 °C. These confirm the existences of a remaining interlayer oxide with a thickness of approximately 5 nm for C1020 and AA1050, after the high-velocity cold-sprayed TiO_2 impacted the substrates.

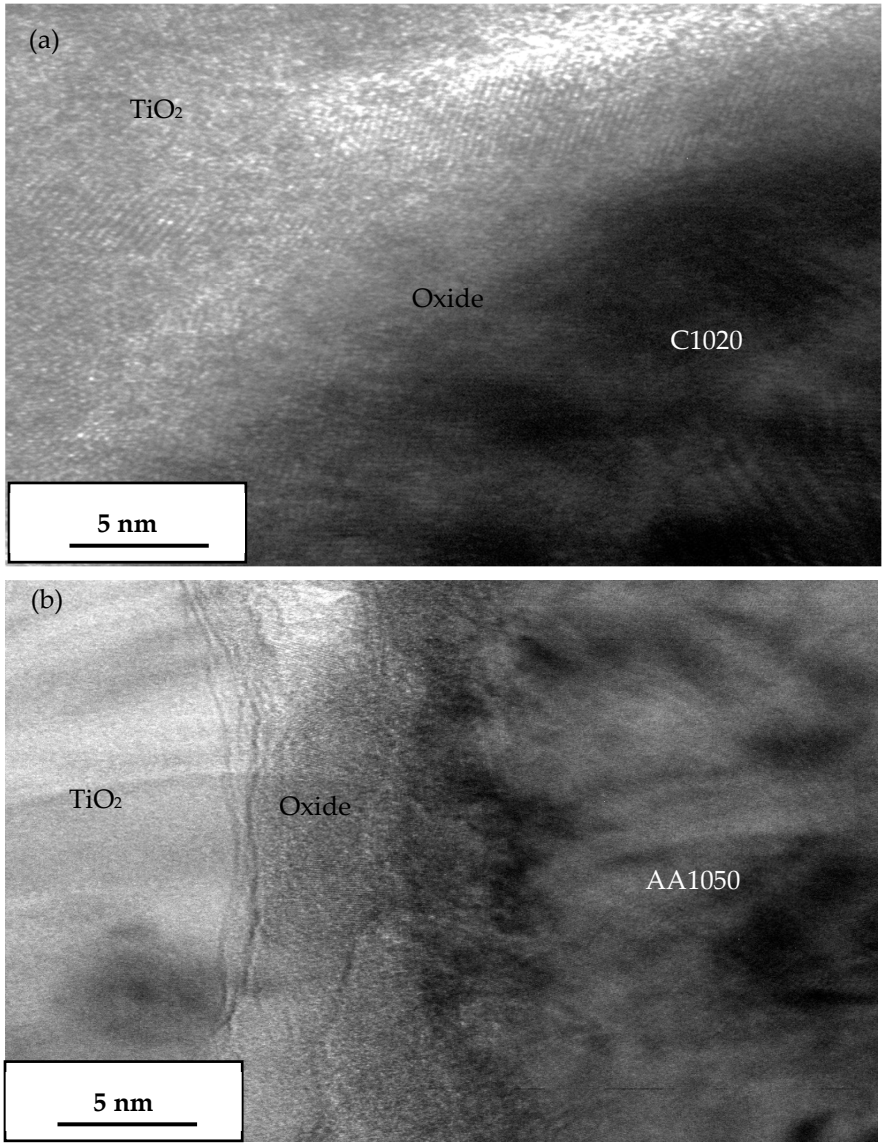

Figure 12. Remaining oxide films at the interface between the TiO_2 particle and (**a**) C1020 and (**b**) AA1050 annealed at 400 °C.

To further understand how the oxide layer remaining on substrate surface plays a role in the bonding mechanism involved between TiO_2 particles and pure metal substrates, TEM line analysis on the single TiO_2 particle on pure metals at room temperature and samples annealed at 400 °C was conducted. Figure 13 is the TEM line analysis results of a single TiO_2 particle on C1020 at room temperature and after 400 °C annealing. These confirm the existence of atomic Ti on room-temperature C1020. On the other hand, for C1020 annealed at 400 °C, the intermixing of Cu, Ti and O is present in the particle area, and there is no trace of atomic Ti on the substrate surface. This may explain why there was no successful coating on C1020 annealed at 400 °C, because of the thicker oxide layer on the substrate surface.

Figure 14 is the TEM line analysis results of a single TiO_2 particle on AA1050 at room temperature and after 400 °C annealing. These confirm the existence of the intermixing of atomic Ti and O on room-temperature AA1050. On the other hand, in AA1050 annealed at 400 °C, only a higher atomic percentage of O was present, due to the annealing process. This created a more inactive area for TiO_2 particles to bond on the substrate surface. At the atomic level, metallurgical bonding is thought to be the result of a chemical reaction of particles or particle/substrate at the oxide-free contact [7,32–34]. Metallurgical bonding

could occur when two fresh metallic areas come into atomic interaction. Therefore, bonding necessitates at least some breaking up of the native oxide film, meaning that the thicknesses of this layer may influence the critical velocity. Dedicated studies are required to develop a straightforward relationship between oxide film thickness and the critical velocity [35]. According to the findings of this study, the main factor is the atomic reaction between sprayed TiO_2 particles and newly formed substrate material of pure copper and pure aluminum; this is metallurgical bonding, which is similar to the cold spraying of metallic materials.

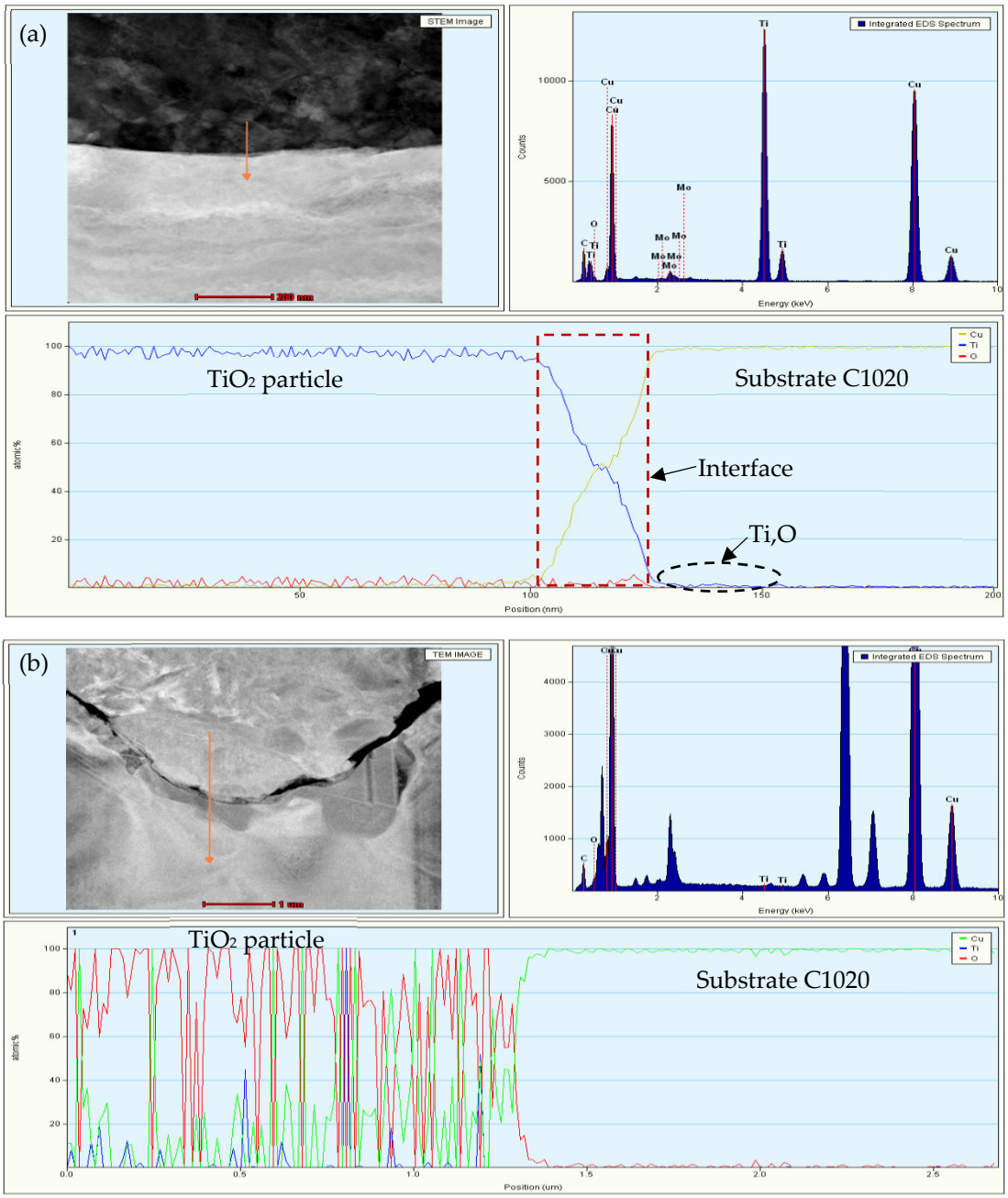

Figure 13. TEM line analysis of the TiO_2 particle on C1020 (**a**) at RT and (**b**) annealed at 400 °C.

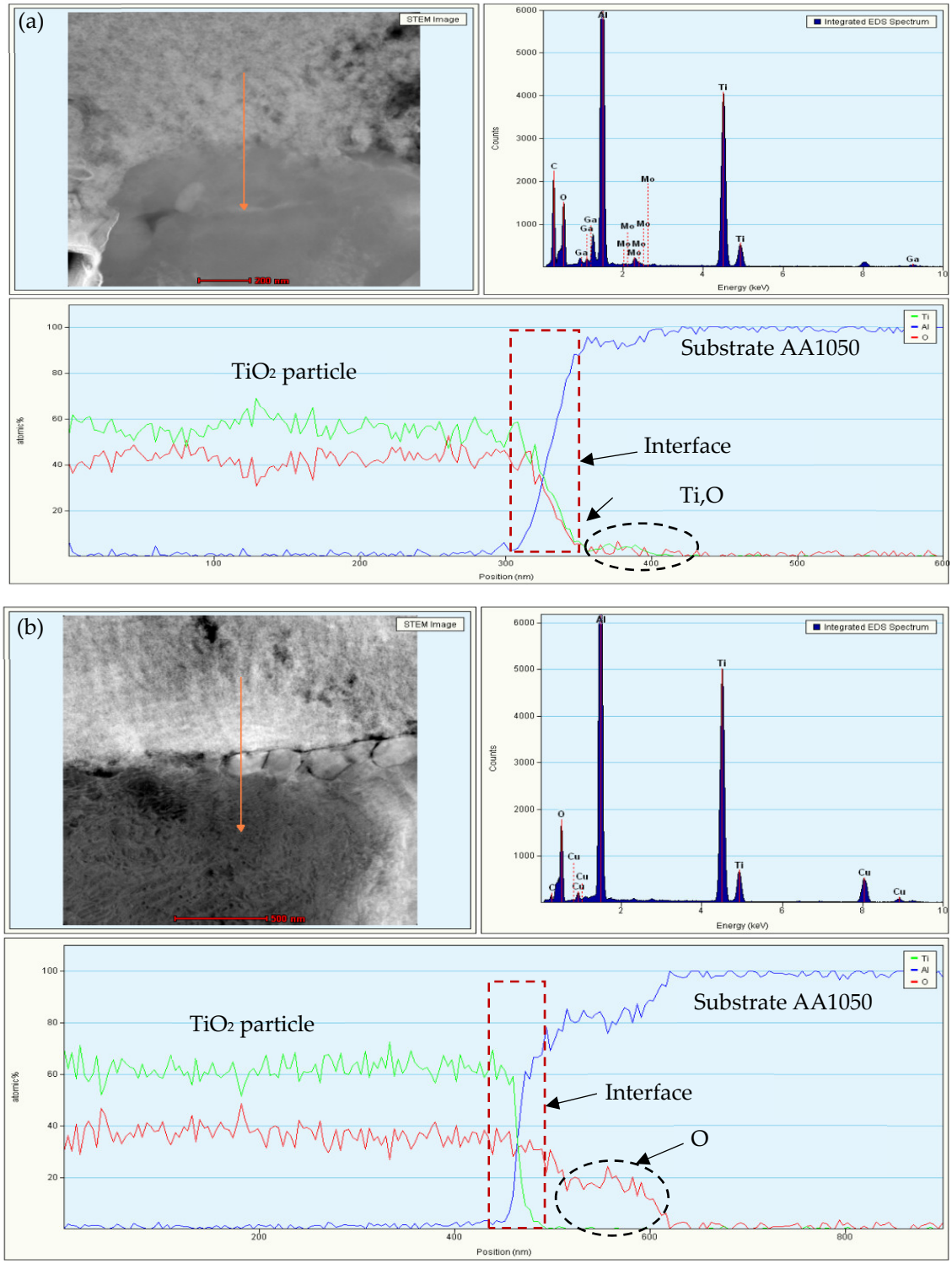

Figure 14. TEM line analysis of the TiO_2 particle on AA1050 (**a**) at RT (**b**) annealed at 400 °C.

3.8. Adhesion Strength on Substrate Annealed at 400 °C Surface Condition

Figure 15 shows the cold-sprayed titanium dioxide coating bond strength on C1020 and AA1050 substrates annealed at 400 °C with and without an oxide on the substrate surface. No oxide layer here means that the C1020 and AA1050 were subjected to annealing in electric furnace, then grit-blasted before the cold-spraying process. Grit blasting is a surface treatment for cleaning or roughening. Both soft substrates annealed at 400 °C with no oxidation exhibited an increasing trend in the adhesion strength of cold-sprayed

TiO_2 coatings compared to an oxidized substrate, which was N/A to 1.44 MPa for C1020 and 2.61 to 4.93 MPa for AA1050. From this result, it clearly indicates that the main factor which influences the bond strength of cold-sprayed titanium dioxide coatings is the remaining substrate oxidation which is not fully removed after strong impacts from cold-sprayed TiO_2. At the atomic level, metallurgical bonding is thought to be the result of a chemical reaction of particles or particle/substrate at the oxide-free interface [7,32–34]. Referring to the findings, the chemical reactions among cold-sprayed TiO_2 particles and the new surface of pure metal substrates which are oxide-free are thought to be the most important factor. Overall, the adhesion strength of the TiO_2 coating on AA1050 was higher compared to C1020 in all conditions, due to aluminum's reduced hardness when compared to copper. Oxide forms were also different on both pure metals, which may have influenced the coating strength of the cold-sprayed titanium dioxide coating on both substrate materials. Figure 16 shows a schematic image of cold-sprayed TiO_2 deposition onto soft substrate materials, with a thin oxide layer at room temperature and thick oxide layer after annealing.

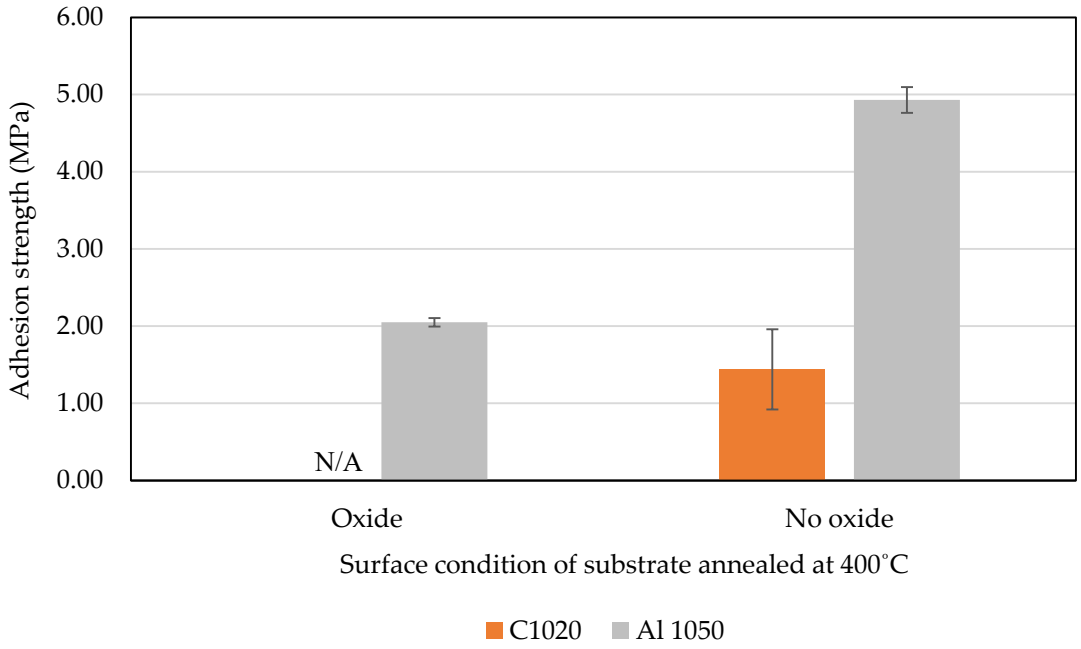

Figure 15. Cold-sprayed titanium dioxide coating bond strength on C1020 and AA1050 annealed at 400 °C.

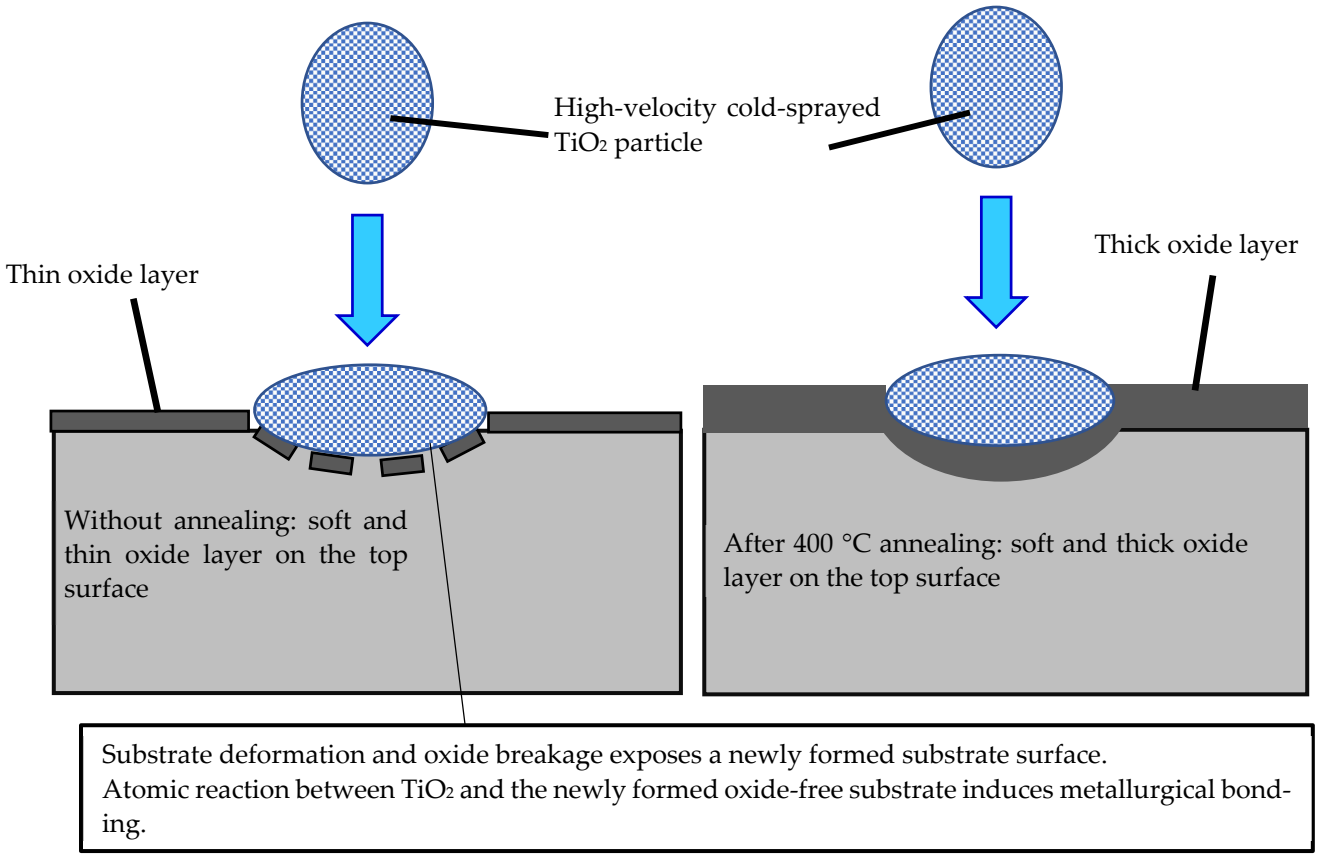

Figure 16. Schematic image of cold-sprayed TiO_2 deposition onto soft materials with thin and thick oxide layers.

4. Conclusions

Herein, we examined the impact of the bond strength of cold-sprayed titanium dioxide on pure copper (C1020) and pure aluminum (AA1050) through substrate properties that are annealed in an electrical furnace temperature range from ambient temperature to 400 °C. The following is a summary of the study's findings:

1. The annealing process contributed to the induced ductility of C1020 and AA1050, especially when annealed at a recrystallization temperature of 400 °C. The substrate's hardness was reduced as a result, and it became softer. When the high-velocity cold-sprayed TiO_2 particle struck the pure metals annealed at 400 °C with an oxide film, plastic deformation of the substrate is present, but some of the oxide layer remained, as shown by the TEM results, which prevented metallurgical bonding from occurring in between the TiO_2 coating and pure metals;
2. Metallurgical bonding of cold-sprayed TiO_2 particles and newly created oxide-free pure metal surfaces is the primary bonding mechanism.

Author Contributions: Conceptualization and methodology, N.i.O.; formal analysis, investigation, data curation and writing—original draft preparation, N.i.O.; writing—review and editing, M.Y.; supervision, T.Y., M.Y. and M.F.; funding acquisition, M.Y. All authors have read and agreed to the published version of the manuscript.

Funding: This research is supported by JSPS KAKENHI Grant Number JP17K06857 and was partially carried out at the Cooperative Research Facility Center at Toyohashi University of Technology.

Institutional Review Board Statement: Not applicable.

Informed Consent Statement: Not applicable.

Data Availability Statement: Not applicable.

Acknowledgments: We acknowledge the Interface & Surface Fabrication Lab.Toyohashi University of Technology, Majlis Amanah Rakyat,MARA and Universiti Teknikal Malaysia Melaka,UTeM for Noor Irinah's scholarship.

Conflicts of Interest: The authors declare no conflict of interest.

References

1. PPapyrin, A.; Kosarev, V.; Klinkov, S.; Alkhimov, A.; Fomin, V.M. *Cold Spray Technology*; Elsevier: Amsterdam, The Netherlands, 2006; pp. 70–96.
2. Champagne, V.K. *The Cold Spray Materials Deposition Process Fundamentals and Applications*, 1st ed.; Victor, K.C., Ed.; Woodhead Publishing Limited: Cambridge, UK, 2007; pp. 132–149.
3. Assadi, H.; Gärtner, F.; Stoltenho, T.; Kreye, H. Bonding mechanism in cold gas spraying. *Acta Mater.* **2003**, *51*, 4379–4394.
4. Assadi, H.; Schmidt, T.; Richter, H.; Kliemann, J.-O.; Binder. K.; Klassen, F.; Kreye. H. On Parameter Selection in Cold Spraying. *J. Therm. Spray Technol*. **2011**, *20*, 1161–1176.
5. Grujicic, M.; Zhao, C.I.; De Rosset, W.S.; Helfritch, D. Adabatic shear instability-based mechanism for article/substrate bonding in the cold-gas dynamic-spray process. *Mater. Des*. **2004**, *25*, 681–688.
6. Villafuerte, J. *Modern Cold Spray: Materials, Process, and Applications,* 1st ed.; Villafuerte, J., Ed.; Springer: Windsor, ON, Canada, 2015; pp. 1–6.
7. Moridi, A.; Hassani-Gangaraj, S.M.; Guagliano, M.; Dao, M. Cold spray coating: Review of material systems and future perspectives. *Surf. Eng*. **2014**, *30*, 369–395.
8. Chromik, R.R.; Alidokht, S.A.; Shockley, J.M.; Zhang, Y. Tribological Coatings Prepared by Cold Spray. In *Cold-Spray Coatings: Recent Trends and Future Perspectives*; Cavaliere, P., Ed.; Springer: Lecce, Italy, 2018; pp. 321–348.
9. Hench, L.L.; Best, S.M. Ceramics, Glasses, and Glass Ceramics: Basic Principles. In *Biomaterials Science*; Academic Press: Lodon, UK, 2013; pp. 128–151.
10. Shahid, H.; Xiaoyong, Y.; Muhammad Kashif, A.; Asma, S.; Muhammad Sufyan, J.; Nimra, A.; Bilal, A.; Guiwu, L.; Guanjun, Q. Robust TiN Nanoparticles Polysulfide Anchor for Li–S Storage and Diffusion Pathways Using First Principle Calculations. *Chem. Eng. J.* **2020**, *391*, 123595.
11. Shahid, H.; Abdul Jabbar, K.; Muhammad, A.; Muhammad Sufyan, J.; Awais, A.; Syed Shoaib, A.S.; Mohammad Rizwan, K.; Shakeel, A.; Zulfiqar; Shafaqat, A.; Zeid, A.A.L.O.; et al. Charge storage in binder-free 2D-hexagonal $CoMoO_4$ nanosheets as a redox active material for pseudocapacitors. *Ceram. Intern*. **2021**, *47*, 8659–8667.
12. Shahid, H.; Mobashar, H.; Muhammad Sufyan, J.; Asma, S.; Syed Shoaib, A.S.; Muhammad Tariq, N.; Tayyba, N.; Abdul Jabbar, K.; Xiangzhao, Z.; Guiwu, L. Distinctive flower-like CoNi2S4 nanoneedle arrays (CNS–NAs) for superior supercapacitor electrode performances. *Ceram .Intern*. **2020**, *46*, 25942–25948.
13. Yamada, M.; Kandori, Y.; Sato, K.; Fukumoto, M. Fabrication of Titanium Dioxide Photocatalyst Coatings by Cold Spray. *J. Solid Mech. Mater. Eng.* **2009**, *3*, 210–216.
14. Yamada, M.; Isago, H.; Nakano, H.; Fukumoto, M. Cold spraying of TiO_2 photocatalyst coating with nitrogen process gas. *J. Therm. Spray Technol.* **2010**, *19*, 1218–1223.
15. Salim, N.T.; Yamada, M.; Nakano, H.; Shima, K.; Isago, H.; Fukumoto, M. The effect of post-treatments on the powder morphology of titanium dioxide (TiO_2) powders synthesized for cold spray. *Surf. Coat. Technol*. **2011**, *206*, 366–371.
16. Toibah, A.R.; Sato, M.; Yamada, M.; Fukumoto, M. Cold-Sprayed TiO_2 Coatings from Nanostructured Ceramic Agglomerated Powders. *Mater. Manuf. Process.* **2016**, *31*, 1527–1534.
17. Toibah, A.R.; Takahashi, K.; Yamada, M.; Fukumoto, M. Effect of Powder Calcination on the Cold Spray Titanium Dioxide Coating. *Mater. Trans.* **2016**, *57–58*, 1345–1350.
18. Winnicki, M.; Latka, L.; Jasiorski, M.; Baszczuk, A. Mechanical properties of TiO_2 coatings deposited by low pressure cold spraying. *Surf. Coat Technol*. **2020**, *405*, 126516.
19. Schmidt, K.; Buhl, S.; Davoudi, N.; Godard, C.; Merz, R.; Raid, I.; Kerscher, E.; Kopnarski, M.; Renno, C.M.; Ripperger, S.; et al. Ti surface modification by cold spraying with TiO_2 mircoparticles. *Surf. Coat. Technol*. **2017**, *309*, 749–758.
20. Kliemann, J.-O.; Gutzmann, H.; Gärtner, F.; Hübner, H.; Borchers, C.; Klassen, T. Formation of cold-sprayed ceramic titanium dioxide layers on metal surfaces. *J. Therm. Spray Technol.* **2010**, *20*, 292–298.
21. Gutzmann, H.; Freese, S.; Gartner, F.; Klassen, T. Cold gas spraying of ceramics using the example of titanium dioxide. In Proceedings of the International Thermal Spray Conference, ITSC, Hamburg, Germany, 27–29 September 2011; pp. 391–396.
22. Gardon, M.; Fernández-Rodíguez, C.; Garzón Sousa, D.; Doña-RodRíguez, J.M.; Dosta, S.; Cano, I.G.; Guilemany, J.M. Photocatalytic activity of nanostructured anatase coatings obtained by cold gas spray. *J. Therm. Spray Technol.* **2014**, *23*, 1135–1140.
23. Li, W.-Y.; Li, C.-J.; Liao,H. Significant influence of particle surface oxidation on deposition efficiency, interface microstructure and adhesive strength of cold-sprayed copper coatings. *Appl. Surf. Sci.* **2010**, *256*, 4953–4958.
24. Kumar, S.; Bae, G.; Lee, C. Deposition characteristics of copper particles on roughened substrates through kinetic spraying. *Appl. Surf. Sci.* **2009**, *255*, 3472–3479.
25. Richer, P.; Jodoin, B.; Ajdelsztajn, L.; Lavernia, E.J. Substrate roughness and thickness effects on cold spray nanocrystalline Al–Mg coatings. *J. Therm. Spray Technol.* **2006**, *15*, 246–254.

26. Mäkinen, H.; Lagerbom, J.; Vuoristo, P. Adhesion of Cold Sprayed Coatings: Effect of Powder, Substrate, and Heat Treatment. In Proceedings of the Thermal Spray 2007: Global Coating Solutions, Beijing, China, 14–16 May 2007, Marple, B.R., Hyland, M.M., Lau, Y.-C., Li, C.-J., Lima, R.S., Montavon, G., Eds.; ASM International: 2007; pp. 31–36.
27. Clayton, C.R. Materials science and engineering: An introduction. *Mater. Sci. Eng.* **1987**, *94*, 266–267.
28. Benchabanea, G.; Boumerzouga, Z.; Thibonb, I.; Gloriantb, T. Recrystallization of pure copper investigated by calorimetry and microhardness. *Mater. Charact.* **2008**, *59*, 1425–1428.
29. Ernst, K.-R.; Braeutigam, J.; Gaetner, F.; Klassen, T. Effect of substrate temperature on cold-gas-sprayed coatings on ceramic substrates. *J. Therm. Spray Technol.* **2013**, *22*, 422–432.
30. Ichikawa, Y.; Ogawa, K. Effect of Substrate Surface Oxide Film Thickness on Deposition Behavior and Deposition Efficiency in the Cold Spray Process. *J. Therm. Spray Technol*. **2015**, *24*, 1269–1276.
31. Ichikawa, Y.; Tokoro, R.; Tanno. M.; Ogawa, K. Elucidation of cold-spray deposition mechanism by auger electron spectroscopic evaluation of bonding interface oxide film. *Acta Mater.* **2019**, *164*, 39–49.
32. Irissou, E.; Legoux, J.G.; Ryabinin, A.N.; Jodoin, B.; Moreau, C. Review on Cold Spray Process and Technology: Part I—Intellectual Property. *J. Therm. Spray Technol.* **2008**, *17*, 495–516.
33. Goldbaum, D.; Poirier, D.; Irissou, E.; Legoux, J.G.; Moreau, C. Review on cold spray process and technology US patents. In *Modern Cold Spray*; Springer, Cham, Switzerland, 2015; pp. 403–429.
34. Grigoriev, S.; Okunkova, A.; Sova, A.; Bertrand, P.; Smurov, I. Cold spraying: From process fundamentals towards advanced applications. *Surf. Coats Technol.* **2015**, *268*, 77–84.
35. Mostafa, H.-G.; David, V.; Keith, A.N.; Christopher, A.S. Impact-bonding with aluminum, silver, and gold microparticles: Toward understanding the role of native oxide layer. *Appl. Surf. Sci.* **2019**, *476*, 528–532.